Optimal photon polarization toward the observation of the nonlinear Breit-Wheeler pair production

Yunquan Gao and Suo Tang*

College of Physics and Optoelectronic Engineering, Ocean University of China, Qingdao, Shandong 266100, China

(Received 3 July 2022; accepted 21 August 2022; published 6 September 2022)

We investigate the optimization of the photon polarization to increase the yield of the Breit-Wheeler pair production in arbitrarily polarized plane wave backgrounds. We show that the optimized photon polarization can improve the positron yield by more than 20% compared to the unpolarized case, in the intensity regime of current laser-particle experiments. The seed photon's optimal polarization is the result of the polarization coupling with the polarization of the laser pulse. The compact expressions of the coupling coefficients in both the perturbative and nonperturbative regimes are given. Because of the evident difference in the coupling coefficients for the linear- and circular-polarization components, the seed photon's optimal polarization state in an elliptically polarized laser background deviates considerably from the orthogonal state of the laser polarization.

DOI: 10.1103/PhysRevD.106.056003

I. INTRODUCTION

The production of an electron-positron pair in the collision of two high-energy photons, now referred to as the linear Breit-Wheeler process (LBW), was first proposed in the 1930s [1]. The production yield depends not only on the photons' dynamical parameters, but also on the relative polarization of the two photons [1–3].

With the improvement of the laser intensity, the decay of a single high-energy photon into an electron-positron pair in the collision with an intense laser pulse, which is often referred to as the nonlinear Breit-Wheeler (NBW) pair production [4–7], has been measured in the multiphoton perturbative regime via the landmark E144 experiment more than two decades ago [8,9] and has been broadly studied within different types of laser fields [10–23]. The dependence of the NBW process on the polarization state of the seed photon has also been partially investigated in the current literature [24–33], in which the laser backgrounds are commonly specified with the pure linear and/or circular polarization, and the production yield could be considerably improved/suppressed when the polarization of the seed photon is set to be orthogonal/parallel to that of the background field [30–33]. However, in an arbitrarily polarized laser background, how to assign the photon polarization to acquire the maximal production yield has not been clearly investigated.

In the LBW process, the polarization dependence of the production is the result of the polarization coupling between the two high-energy photons [1–3]. However, how the polarization of the seed photon couples with that of the laser pulse (or multiple laser photons) in the NBW process is still not clear. In this paper, we concentrate on the properties of the polarization coupling between the seed photon and the laser pulse and reveal the optimal polarization of the seed photon for the maximal yield of the NBW process in arbitrarily polarized laser backgrounds. We find that the linear- and circular-polarization components of the seed photon couple with the corresponding components of the laser polarization with quite different coefficients, and thus in an elliptically polarized laser pulse, the optimal polarization state of the seed photon deviates considerably from the orthogonal state of the laser polarization.

The study of the optimal photon polarization for the maximal production yield is partly motivated by the upcoming high-energy laser-particle experiments, i.e., LUXE at DESY [34–37] and E320 at SLAC [38–41] in which beams of photons with energy $O(10\ \mathrm{GeV})$ are generated to collide with laser pulses with intermediate intensity $\xi \sim O(1)$, and one of their main goals is to detect the NBW process in the transition regime from the perturbative to the nonperturbative regime [36,37], where ξ is the classical nonlinearity parameter for laser intensity. In this planned intensity regime, the production yield could be enhanced/suppressed considerably by the photon polarization effect [30,33], and by measuring the production yield from differently polarized photons, the polarization

*tangsuo@ouc.edu.cn

coupling effect may also be detectable in these upcoming experiments.

The paper is organized as follows. The theoretical model and relevant parameters are introduced in Sec. II. In Sec. III, we first explore the perturbative intensity regime and discuss the photon polarization coupling in the LBW process, and then, we go to the nonperturbative intensity regime to discuss the polarization coupling between the seed photon and the laser pulse in the NBW process in Sec. IV. At the end, we conclude in Sec. V. In the following discussions, the natural units $\hbar = c = 1$ is used, and the fine structure constant is $\alpha = e^2 \approx 1/137$.

II. THEORETICAL MODEL

We consider the typical scenario in the modern-day laser-particle experiments in which a beam of high-energy photons interacts with an intense laser pulse in the geometry close to the head-on collision. The laser pulse is modeled as a plane wave with scaled vector potential $a^\mu(\phi) = |e|A^\mu(\phi)$ depending only on the laser phase $\phi = k \cdot x$, where $k^\mu = \omega(1, 0, 0, -1)$ is the laser wave vector, ω is the central frequency of the laser pulse, and $|e|$ is the charge of the positron. This plane wave background is a good approximation for the collision between a high-energy particle and a weakly focused pulse [10,42–45]. The collision is characterized by the energy parameter $\eta = k \cdot \ell/m^2$ and laser intensity parameter ξ, where ℓ^μ is the photon momentum and m is the electron rest mass.

The total yield of the NBW pair production from a polarized seed photon can be acquired via the standard S-matrix approach [33] or by taking the imaginary part of the polarization operator [46], and can be given as

$$\begin{aligned} P = \frac{\alpha}{(2\pi\eta)^2} \int \frac{\mathrm{d}s}{ts} \int \mathrm{d}^2\boldsymbol{r} \iint \mathrm{d}\phi_1 \mathrm{d}\phi_2 \, e^{i\int_{\phi_2}^{\phi_1} \mathrm{d}\phi' \frac{\ell\cdot\pi_q(\phi')}{m^2\eta t}} \\ \times \{h_s \boldsymbol{\Delta}^2/2 + 1 - i h_s \Gamma_3 \boldsymbol{w}(\phi_1) \times \boldsymbol{w}(\phi_2) \\ - \Gamma_1 [w_x(\phi_1) w_x(\phi_2) - w_y(\phi_1) w_y(\phi_2)] \\ - \Gamma_2 [w_x(\phi_1) w_y(\phi_2) + w_y(\phi_1) w_x(\phi_2)]\}, \end{aligned} \tag{1}$$

where $\boldsymbol{\Delta} = i[\boldsymbol{a}^\perp(\phi_1) - \boldsymbol{a}^\perp(\phi_2)]/m$, $h_s = (s^2 + t^2)/(2st)$, $\boldsymbol{w}(\phi) = \boldsymbol{r} - \boldsymbol{a}^\perp(\phi)/m$, and $\boldsymbol{w}(\phi_1) \times \boldsymbol{w}(\phi_2) = w_x(\phi_1) \times w_y(\phi_2) - w_y(\phi_1) w_x(\phi_2)$, $s = k \cdot q/k \cdot \ell$ ($t = 1 - s$) is the fraction of the light front momentum taken by the produced position (electron), and $\boldsymbol{r} = (\boldsymbol{q}^\perp - s\boldsymbol{\ell}^\perp)/m$ denotes the transverse momenta of the positron, and $\pi_q(\phi)$ is the positron's instantaneous momentum in the laser pulse:

$$\pi_q^\mu(\phi) = q^\mu - a^\mu(\phi) + \frac{q \cdot a(\phi)}{k \cdot q} k^\mu - \frac{a^2(\phi)}{2k \cdot q} k^\mu.$$

The polarization of the seed photon is comprehensively described with the classical Stokes parameters $(\Gamma_1, \Gamma_2, \Gamma_3)$ [47,48]: Γ_1 (Γ_2) is the degree of linear polarization indicating the preponderance of the polarization in the ε_x state (ε_{45° state) over that in the ε_y state (ε_{135° state), and Γ_3 is the degree of circular polarization giving the preponderance of the polarization in the ε_+ state over that in the ε_- state. The polarization bases are given as

$$\begin{aligned} \epsilon_x^\mu &= \epsilon_x^\mu - \frac{\ell \cdot \epsilon_x}{k \cdot \ell} k^\mu, \qquad \epsilon_y^\mu = \epsilon_y^\mu - \frac{\ell \cdot \epsilon_y}{k \cdot \ell} k^\mu, \\ \epsilon_\psi^\mu &= \epsilon_\psi^\mu - \frac{\ell \cdot \epsilon_\psi}{k \cdot \ell} k^\mu, \qquad \epsilon_\pm^\mu = \epsilon_\pm^\mu - \frac{\ell \cdot \epsilon_\pm}{k \cdot \ell} k^\mu, \end{aligned}$$

where $\epsilon_x^\mu = (0, 1, 0, 0)$, $\epsilon_y^\mu = (0, 0, 1, 0)$ and $\epsilon_\psi = \epsilon_x \cos\psi + \epsilon_y \sin\psi$, $\epsilon_\pm = (\epsilon_x \pm i\epsilon_y)/\sqrt{2}$. For fully polarized photon beams, the Stokes parameters satisfy $\Gamma_1^2 + \Gamma_2^2 + \Gamma_3^2 = 1$ and for partially polarized photon beams, $\Gamma_1^2 + \Gamma_2^2 + \Gamma_3^2 < 1$. The full definition of the photon Stokes parameters $(\Gamma_1, \Gamma_2, \Gamma_3)$ can be found in Ref. [33].

Based on (1), the total yield of the NBW process can be expressed in form as

$$P = n_0 + \Gamma_1 n_1 + \Gamma_2 n_2 + \Gamma_3 n_3, \tag{2}$$

where n_0 is the unpolarized contribution independent on the photon polarization ($\Gamma_{1,2,3} = 0$) [22,23], and $n_{1,2,3}$ denote the contributions coupling to the polarization of the seed photon. As one can simply infer, to maximize the production yield

$$P_m = n_0 + n_p, \tag{3}$$

the photon polarization should be selected as

$$(\Gamma_1, \Gamma_2, \Gamma_3) = (n_1, n_2, n_3)/(n_1^2 + n_2^2 + n_3^2)^{1/2}, \tag{4}$$

which prompts the existence of the optimal photon polarization for the specified laser pulse and collision parameter η to achieve the maximal production yield, where $n_p = (n_1^2 + n_2^2 + n_3^2)^{1/2}$ is the maximal contribution from the photon polarization. If one reverses the optimal polarization of the seed photon, i.e., $\Gamma_{1,2,3} \to -\Gamma_{1,2,3}$, the pair production would be largely suppressed.

III. LINEAR BREIT-WHEELER PROCESS

One may realize that the polarization contribution $\Gamma_i n_i$ in (2) comes from the polarization coupling between the seed and laser photons, and thus the optimal photon polarization (4) depends on the polarization of the laser photons. To manifest this polarization coupling effect, we resort to the perturbative approximation of (1), which is often referred to as the LBW process, by expanding the integrand in (1), keeping only the $\mathcal{O}(\xi^2)$ terms and integrating over s,

$$\begin{aligned} P_\ell = \frac{\pi\alpha^2 \lambda\!\!\!^{-2}_e}{2} \int_{\nu_*}^{+\infty} \mathrm{d}\nu \, D(\nu) \\ \times \{\Xi + \kappa_c \Gamma_3 \varsigma_3(\nu) + \kappa_l [\Gamma_1 \varsigma_1(\nu) + \Gamma_2 \varsigma_2(\nu)]\}, \end{aligned} \tag{5}$$

where $\nu_* = 2/\eta$ is the frequency threshold of the laser photon required to trigger the pair production, $D(\nu) = \nu|\tilde{\boldsymbol{a}}(\nu)|^2/(4\pi^2\alpha\lambda\!\!\!^{-2}_e m^2)$ is the (areal) number density of the laser photon with the frequency $\nu\omega$, $\lambda\!\!\!^{-}_e = 1/m = 386.16$ fm is the electron's reduced Compton wavelength $\tilde{\boldsymbol{a}}(\nu) = \int \mathrm{d}\phi[a_x(\phi), a_y(\phi)]\exp(i\nu\phi)$, and

$$\begin{aligned}\varsigma_1(\nu) &= \frac{|\tilde{a}_x(\nu)|^2 - |\tilde{a}_y(\nu)|^2}{|\tilde{\boldsymbol{a}}(\nu)|^2},\\ \varsigma_2(\nu) &= \frac{\tilde{a}_x^*(\nu)\tilde{a}_y(\nu) + \tilde{a}_x(\nu)\tilde{a}_y^*(\nu)}{|\tilde{\boldsymbol{a}}(\nu)|^2},\\ \varsigma_3(\nu) &= i\frac{\tilde{a}_x(\nu)\tilde{a}_y^*(\nu) - \tilde{a}_x^*(\nu)\tilde{a}_y(\nu)}{|\tilde{\boldsymbol{a}}(\nu)|^2}\end{aligned} \tag{6}$$

are the classical Stokes parameters of the laser photon $\nu\omega$ [48] satisfying $\varsigma_1^2(\nu) + \varsigma_2^2(\nu) + \varsigma_3^2(\nu) = 1$ as the laser photon stays in the coherent polarization state. Similar as the seed photon, $\varsigma_{1,2,3}(\nu)$ characterize the polarization property of the laser photon: $\varsigma_1(\nu)$ $[\varsigma_2(\nu)]$ describes the preponderance of the ϵ_x (ϵ_{45°)-linear polarization over the ϵ_y (ϵ_{135°)-linear polarization, and $\varsigma_3(\nu)$ denotes the preponderance of the ϵ_+-circular polarization over the ϵ_--circular polarization. The parameter

$$\Xi = (1-\beta^2)\left[(3-\beta^4)\ln\left(\frac{1+\beta}{1-\beta}\right) - 2\beta(2-\beta^2)\right] \tag{7}$$

is the contribution from the unpolarized photon [49,50], and

$$\kappa_c = 2(1-\beta^2)\left[\ln\left(\frac{1+\beta}{1-\beta}\right) - 3\beta\right], \tag{8}$$

$$\kappa_l = -\frac{(1-\beta^2)^3}{2}\left[\ln\left(\frac{1+\beta}{1-\beta}\right) + \frac{2\beta}{1-\beta^2}\right] \tag{9}$$

are, respectively, the circular- and linear-polarization coupling coefficients, and indicate the amplitude of the contributions from two kinds of polarization couplings between the seed and laser photon, where $\beta = (1-\nu_*/\nu)^{1/2}$ is actually the normalized velocity of the produced particles in the center-of-mass frame. Equation (5) is actually the integral of the LBW cross section over the energy distribution $D(\nu)$ of the laser photons.

In (5), we can clearly see the contributions from the polarization coupling between the seed and laser photon to the LBW cross section. To maximize the polarization contribution, the polarization of the seed photon is optimized, based on the polarization of the laser photon as

$$[\Gamma_1(\nu), \Gamma_2(\nu), \Gamma_3(\nu)] = \frac{\hat{\kappa}_l[\varsigma_1(\nu), \varsigma_2(\nu), \sigma_l\varsigma_3(\nu)]}{[\varsigma_1^2(\nu) + \varsigma_2^2(\nu) + \sigma_l^2\varsigma_3^2(\nu)]^{1/2}} \tag{10}$$

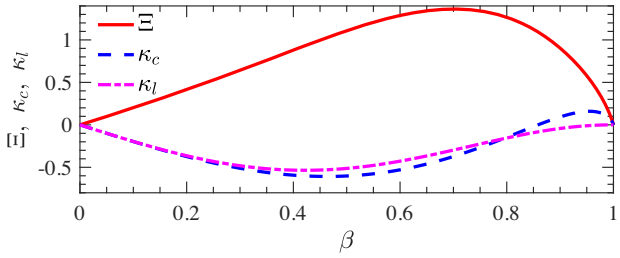

FIG. 1. Comparison between the polarization contributions $\kappa_{c,l}$ and the unpolarized contribution Ξ with the change of the parameter β in the linear Breit-Wheeler process. β is defined in the text and can be simply understood as the normalized velocity of the produced particles in the center-of-mass frame.

where $\hat{\kappa}_l$ is the sign of κ_l, and $\sigma_l = \kappa_c/\kappa_l$ implies the nontrivial dependence of the optimal polarization on the energy of the laser photon in the LBW process. As we can also see in (5), the two sets of linear polarizations have the identical coupling coefficient κ_ℓ, because of the symmetry by rotating the linear-polarization axis 45°. This identity results in the orthogonality between the linear-polarization components of the seed and laser photon as $[\Gamma_1(\nu), \Gamma_2(\nu)] \sim -[\varsigma_1(\nu), \varsigma_2(\nu)]$ as shown in (10) where $\hat{\kappa}_l = -1$ is obtained in Fig. 1.

In Fig. 1, the unpolarized contribution Ξ and the polarization coupling coefficients $\kappa_{l,c}$ are presented with the change of the parameter β. As shown, the polarization contributions are indeed appreciable compared with the unpolarized contribution, especially in the low-energy region $\beta < 0.2$, where $\Xi \approx -\kappa_c \approx -\kappa_l$ and the energy of the laser photon is close to the frequency threshold $\nu \to \nu_*$. With the proper photon polarization, the production could be doubled if $\boldsymbol{\Gamma}\cdot\boldsymbol{\varsigma}(\nu) \to -1$ or completely suppressed if $\boldsymbol{\Gamma}\cdot\boldsymbol{\varsigma}(\nu) \to 1$. Similar to the variation of the unpolarized contribution Ξ with $\beta \in (0,1)$ [50], the amplitudes of the coupling coefficients $\kappa_{c,l}$ increase from zero at $\beta = 0$ to the maximum at around $\beta \approx 0.45$ and then fall off again to zero at $\beta = 1$. In the region of $\beta < 0.4$, the two kinds of polarizations have the same coupling coefficient, $\kappa_c \approx \kappa_l$. This means that, to acquire the maximal polarization contribution, the seed photon should be fully polarized in the state orthogonal to that of the laser photon, i.e., $(\Gamma_1, \Gamma_2, \Gamma_3) = -[\varsigma_1(\nu), \varsigma_2(\nu), \sigma\varsigma_3(\nu)]$ with $\sigma_l \approx 1$ in (10). However, in the higher-energy region with $\beta > 0.4$, the difference between κ_c and κ_l becomes considerable, which implies that the highest production yield is acquired from the seed photon polarized in the state deviating from the orthogonal state of the laser photon. Especially in the extremely high-energy region with $\beta > 0.95$ in which κ_l is close to zero and κ_c becomes positive and dominates the polarization contribution, the highest yield appears when the seed and laser photon have the pure circular polarization parallel to each other.

We now know that the polarization coupling between the two photons in the LBW process could contribute

considerably to the production yield and the polarization contributions $n_{1,2,3}$ in (2) are proportional to the Stokes parameters of the laser photon as $n_{1,2} \sim D(\nu)\kappa_l\varsigma_{1,2}(\nu)$ and $n_3 \sim D(\nu)\kappa_c\varsigma_3(\nu)$ with the coupling coefficients $\kappa_{l,c}$ depending only on the dynamic parameter β in the perturbative regime $\xi \ll 1$. While in the upcoming laser-particle experiments [34,39], the laser intensity has increased to the magnitude of $\xi \sim \mathcal{O}(1)$, in which the Breit-Wheeler pair production is in the transition regime from the perturbative to the nonperturbative regime, a high number of laser photons would be involved to satisfy the energy threshold in the center-of-mass frame, and the NBW process would dominate the pair production. The polarization contributions would, therefore, come from the polarization coupling with the laser pulse, i.e., multiple laser photons, but not with a single laser photon, and the coupling coefficients would depend also on the laser intensity and field ellipticity.

IV. NONLINEAR BREIT-WHEELER PROCESS

In this section, we consider the NBW process stimulated by a high-energy photon in the collision with the laser pulse in the intermediate intensity region $\xi \sim \mathcal{O}(1)$. This is the typical setup for the upcoming laser-particle experiment in LUXE [34,37]. To show the polarization effect clearly, we fix the energy parameter η and adjust the relative polarization of the seed photon and laser pulse.

The background laser field is expressed as

$$a^\mu(\theta,\phi) = m\xi\,\mathrm{Re}\{[0,a_x(\theta),a_y(\theta),0]e^{-i\phi}\}f(\phi), \quad (11)$$

where $\mathrm{Re}\{\cdot\}$ means the real part of the argument, $a_x(\theta) = \cos\theta - i\delta\,\sin\theta$, $a_y(\theta) = \sin\theta + i\delta\cos\theta$. $\delta \in [-1,1]$ characterizes not only the rotation of laser field: $\delta/|\delta| = 1$ is the left-hand rotation and $\delta/|\delta| = -1$ is the right-hand rotation, but also the ellipticity $|\delta|$ of the laser pulse. $|\delta| = 0,\ 1$ corresponds, respectively, to the linearly and circularly polarized laser background and $0 < |\delta| < 1$ gives a laser pulse with the elliptical polarization. The semimajor axis of the elliptical laser field is along $(\cos\theta,\sin\theta)$ with the deflection angle $\theta \in [-\pi,\pi]$ in the transverse plane. $f(\phi)$ depicts the envelope of the laser pulse. The polarization of the laser field could also be described with the classical Stokes parameters $(\varsigma_1,\varsigma_2,\varsigma_3)$ [48] as

$$\begin{aligned}
\varsigma_1 &= \frac{|a_x|^2 - |a_y|^2}{|a_x|^2 + |a_y|^2} = \frac{1-\delta^2}{1+\delta^2}\cos 2\theta,\\
\varsigma_2 &= \frac{a_x^* a_y + a_x a_y^*}{|a_x|^2 + |a_y|^2} = \frac{1-\delta^2}{1+\delta^2}\sin 2\theta,\\
\varsigma_3 &= i\frac{a_x a_y^* - a_x^* a_y}{|a_x|^2 + |a_y|^2} = \frac{2\delta}{1+\delta^2},
\end{aligned} \quad (12)$$

where $\varsigma_1^2 + \varsigma_2^2 + \varsigma_3^2 = 1$. The total linear-polarization degree of the laser pulse is given as $\varsigma_l = (\varsigma_1^2 + \varsigma_2^2)^{1/2} = (1-\delta^2)/(1+\delta^2)$, and the laser's circular-polarization degree is given by ς_3. The equivalence between the laser Stokes parameters (12) and those of the laser photon (6) can be seen when we consider a relatively long laser pulse with the slowly varying envelope $f'(\phi) \approx 0$ and $|\tilde{f}(\nu+1)| \ll |\tilde{f}(\nu-1)|$ at $\nu \geq 1$ [23]. The frequency components of the laser pulse can be written approximately as $\tilde{a}^\mu(\nu) \approx m\xi/2\,[0,a_x(\theta),a_y(\theta),0]\tilde{f}(\nu-1)$ and therefore $\varsigma_i \approx \varsigma_i(\nu)$ with $i = 1,2,3$.

A. Numerical results

To show the importance of polarization contributions and their dependence on the corresponding laser Stokes parameters, we first present the numerical results for the NBW process stimulated by a 16.5 GeV photon in the head-on collision with the laser pulse in the intermediate intensity region $\xi \sim \mathcal{O}(1)$. The pulse envelope is given as $f(\phi) = \cos^2[\phi/(4\sigma)]$ in $|\phi| < 2\pi\sigma$ and $f(\phi) = 0$ otherwise, where $\sigma = 8$. The calculations have been done with the laser central frequency $\omega = 4.65$ eV, as an example, which is the third harmonic of the normal laser with the wavelength $\lambda = 0.8\ \mu$m. For the detailed calculation of (1), one can refer to the presentation in Ref. [22] and the analogous calculation in Ref. [51] for the polarized nonlinear Compton scattering.

In Fig. 2, we present the energy spectra of the produced positrons in the laser backgrounds with the same intensity $\xi = 1$ and deflection angle $\theta = 0$ but different ellipticity $\delta = 1, 0.5, 0$ in Figs. 2(a)–2(c) respectively. As shown, the potential contributions coupling to the photon polarization are indeed appreciable for the total positron yield. For the circularly polarized laser background, $\delta = 1$ in Fig. 2(a) with $(\varsigma_1,\varsigma_2,\varsigma_3) = (0,0,1)$, the relative importance of the contribution n_3 coupling to the circular polarization Γ_3 of the seed photon is about $|n_3|/n_0 \approx 22.3\%$ compared to the unpolarized contribution n_0. The contributions $n_{1,2}$ coupling to the photon's linear polarization are zero, because the background field has no linear polarization [33]. By increasing the linear polarization of the background field $(\varsigma_1,\varsigma_2,\varsigma_3) = (0.6,0,0.8)$ in Fig. 2(b) with the ellipticity $\delta = 0.5$, the polarized contribution n_1 becomes important with $|n_1|/n_0 \approx 27.8\%$, while the importance of the polarized contribution n_3 decreases to about $|n_3|/n_0 \approx 14.5\%$. For the laser pulse with the full linear polarization in Fig. 2(c) with $\delta = 0$ and $(\varsigma_1,\varsigma_2,\varsigma_3) = (1,0,0)$, the polarized contribution n_3 becomes zero, and the relative importance of the polarized contribution n_1 increases to about $|n_1|/n_0 \approx 32.6\%$. With the decrease of the laser ellipticity, the harmonic structure becomes more clear in the energy spectra and appears around $s_{n>5} = \{1 \pm [1-(2+\xi^2)/(n\eta)]^{1/2}\}/2$ [33] when $\delta = 0$. The boundary of the

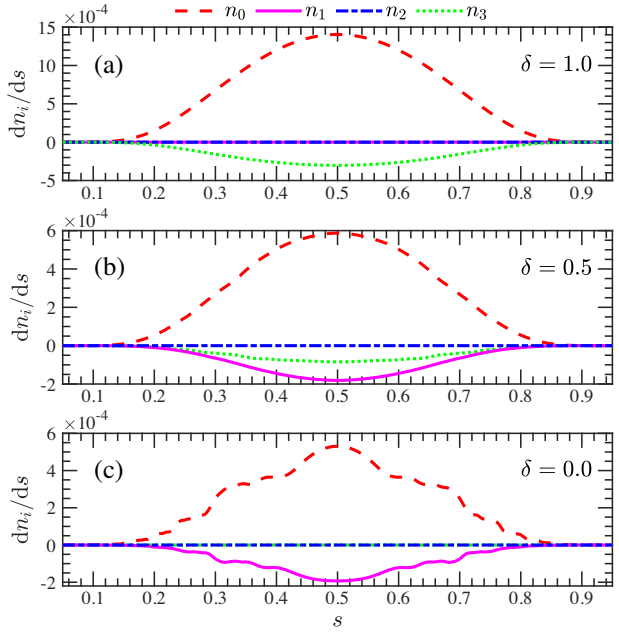

FIG. 2. The energy spectra of the produced positrons via the NBW process in the head-on collision between a polarized photon and the laser pulse with different ellipticity: (a) $\delta = 1$ circular polarization, (b) $\delta = 0.5$ elliptical polarization, and (c) $\delta = 0$ linear polarization. The polarized contributions $n_{1,2,3}$ coupling to the photon polarizations $\Gamma_{1,2,3}$, are compared with the unpolarized contribution n_0. The energy of the seed photon is 16.5 GeV. The laser pulse has the intensity $\xi = 1$, central frequency $\omega = 4.65$ eV, and the deflection angle $\theta = 0$.

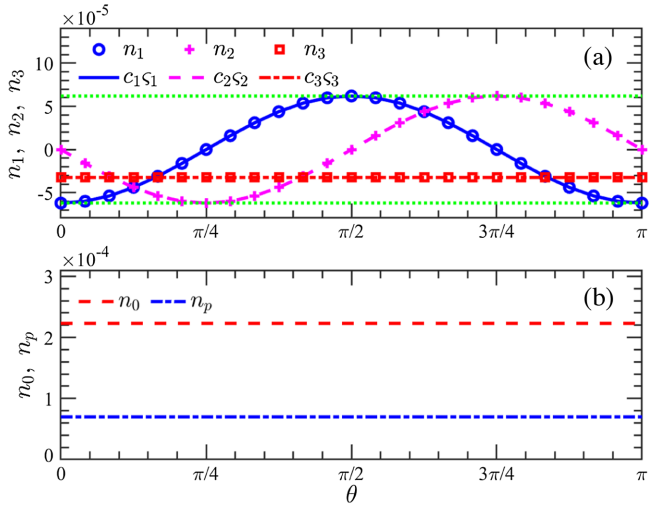

FIG. 3. Different contributions to the positron yield of the NBW process in the elliptically polarized laser pulse with $\delta = 0.5$ and the deflection angle $\theta \in [0, \pi]$. (a) The variation of the polarization contributions $n_{1,2,3}$ with the change of the field deflection angle. The full QED results ("cycle," "plus," and "square") are fitted with the corresponding laser Stokes parameters as $c_{1,2,3}\varsigma_{1,2,3}$, where $c_1 = n_1(\theta = 0)/\varsigma_1(\theta = 0)$, $c_2 = n_2(\theta = \pi/4)/\varsigma_2(\theta = \pi/4)$, and $c_3 = n_3(\theta = 0)/\varsigma_3(\theta = 0)$. The green dotted lines denote the amplitude of the linear-polarization contributions, i.e., $\pm(n_1^2 + n_2^2)^{1/2}$. (b) The unpolarized contribution n_0 and the maximized polarization contribution n_p in (3) from the seed photon with the optimal polarization in (4). The other parameters are the same as in Fig. 2.

harmonic structure is smoothed because of the finite-pulse duration [23].

In Fig. 2, the contribution n_2 is always zero with the change of the laser ellipticity δ. This is because the laser has no polarization preponderance along the direction of $\theta = \pi/4$, i.e., $\varsigma_2 = 0$. To see the effect of the field deflection angle θ, we plot the variation of the polarization contribution n_i with the change of θ in Fig. 3(a) for $\xi = 1$ and $\delta = 0.5$. As shown, the polarization contributions $n_{1,2}$ vary in the trend as $(n_1, n_2) \propto -(\cos 2\theta, \sin 2\theta)$ and n_3 is unchanged for different θ. All are in the same trend as the variation of the corresponding laser Stokes parameters $\varsigma_{1,2,3}$ in (12). We also note that the amplitude of the linearly polarized contribution $(n_1^2 + n_2^2)^{1/2}$ is constant with the change of θ shown as the green dotted lines in Fig. 3(a). Therefore, the maximized polarization contribution n_p in (3) from the optimized polarization (4) is independent of the field's deflection angle θ as shown in Fig. 3(b), in which we also find that the unpolarized contribution n_0 is unchanged for different θ. This is because of the azimuthal symmetry of the interaction geometry. We can thus conclude that, for laser pulses with the fixed ellipticity δ and intensity ξ, the field's deflection angle θ can only alter the relative values of the linear-polarization contributions $n_{1,2}$ with the constant amplitude $(n_1^2 + n_2^2)^{1/2}$, but not change the circularly polarized (n_3) and unpolarized (n_0) contributions. To show the correlation between the polarization contribution n_i and the corresponding laser Stokes parameter ς_i, we fit the numerical results in Fig. 3(a) respectively as $n_1, n_1(\theta = 0)/\varsigma_1(\theta = 0)\varsigma_1$; $n_2, n_2(\theta = \pi/4)/\varsigma_2(\theta = \pi/4)\varsigma_2$; $n_3, n_3(\theta = 0)/\varsigma_3(\theta = 0)\varsigma_3$, and find the precise agreement between the numerical results and data fitting.

In Fig. 4, we show the variation of the different contributions to the positron yield with the change of the laser ellipticity δ for the fixed deflection angle $\theta = \pi/9$ and laser power density $I = 1$, corresponding to 3.84×10^{19} W/cm^2. As shown in Fig. 4(a), both the unpolarized contribution n_0 and the maximized polarization contribution n_p from the optimal polarization (4) [shown in Fig. 5(b)] decrease with the increase of the laser ellipticity δ from 0 to 1. This is because of the decrease of the field intensity $\xi = [2I/(1 + \delta^2)]^{1/2}$. Simultaneously, the relative importance, n_p/n_0, of the maximized polarization contribution decreases from about 31.6% at $\delta = 0$ for a linearly polarized laser pulse to about 22.3% at $\delta = 1$ for the laser pulse with pure circular polarization. For comparison, we also plot the importance of the polarization contribution $n_p' = -(\varsigma_1 n_1 + \varsigma_2 n_2 + \varsigma_3 n_3)$ from the orthogonal state of the laser polarization, which is clearly smaller than that of

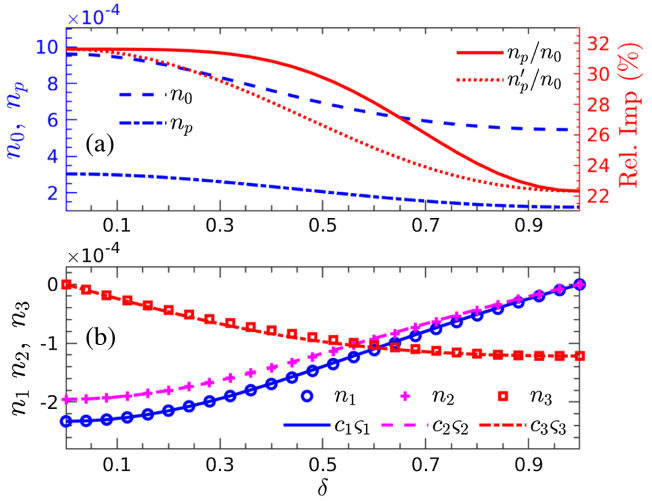

FIG. 4. Different contributions to the positron yield of the NBW process in the laser pulse with different ellipticity $\delta \in [0, 1]$, but with the fixed laser power density $I = \xi^2(1+\delta^2)/2 = 1$ and deflection angle $\theta = \pi/9$. (a) The unpolarized contribution n_0 and the maximized polarization contribution n_p from the seed photon with the optimal polarization in (4). The relative importance n_p/n_0 of the maximal polarization contribution n_p is also plotted and compared with that of the polarization contribution $n'_p = -(\varsigma_1 n_1 + \varsigma_2 n_2 + \varsigma_3 n_3)$ from the photon state orthogonal to the laser polarization. (b) The variation of the polarization contributions $n_{1,2,3}$ with the change of the laser ellipticity. The full QED results (cycle, plus, and square) are fitted with the corresponding laser Stokes parameters as $c_{1,2,3}\varsigma_{1,2,3}$, where $c_{1,2} = n_{1,2}(\delta=0)/\varsigma_{1,2}(\delta=0)$ and $c_3 = n_3(\delta=1)/\varsigma_3(\delta=1)$. The laser power density $I = 1$ corresponds to the real power density $I \approx 3.84 \times 10^{19}$ W cm^{-2}. The other parameters are the same as in Fig. 2.

the optimal polarization state especially for the elliptically polarized laser with $\delta \approx 0.5$. In Fig. 4(b), we see that the amplitudes of the linear-polarization contributions $n_{1,2}$ decrease with the increase of δ, while the amplitude of the contribution from the circular polarization n_3 increases. These variations are again in the same trend as the laser Stokes parameters in (12). The difference between the two linear-polarization contributions can be depicted as $n_1/n_2 \approx \tan 2\theta = \varsigma_1/\varsigma_2$. The numerical results in Fig. 4(b) are respectively fitted as $n_{1,2}, n_{1,2}(\delta=0)/\varsigma_{1,2}(\delta=0)\varsigma_{1,2}$ and $n_3, n_3(\delta=1)/\varsigma_3(\delta=1)\varsigma_3$, and again, we see the agreement between the numerical results and data fitting. The slight difference around $\delta \approx 0.4$ implies the dependence of the polarization coupling between the seed photon and laser pulse on the laser ellipticity, as we will see later.

In this section, we investigate the NBW process in the laser pulse with the ellipticity $\delta \in [0, 1]$ and deflection angle $\theta \in [0, \pi]$. For the laser pulse with the ellipticity $\delta \in [-1, 0]$, the laser field would rotate in the opposite direction of the laser with the ellipticity $-\delta$ (see the expression for ς_3). The calculations would be consistent with the above results, except that the polarized contribution n_3 would change sign, but keep the same amplitude. For the laser pulse with the deflection angle $\theta \in [-\pi, 0]$, all the above results would also be the same except that the polarized contribution n_2 would change sign because of the odd property of ς_2. All the calculations have to be done for a relatively long laser pulse, and for an ultrashort laser pulse, the conclusion would be different as its polarization property could deviate largely from the description of the classical Stokes parameters in Eq. (12).

B. Analytical results in a monochromatic field

To interpret the properties of the polarization coupling between the seed photon and the laser pulse in the NBW process, we resort to the analytical result in an elliptically polarized monochromatic field with $f(\phi) = 1$ in (11), which could work as a good reference for the finite-pulse results discussed above with the slowly varying envelope $f'(\phi) \approx 0$ [52]. After integrating the transverse momenta in (1), we can acquire the polarization contributions as

$$(n_1, n_2, n_3) = \alpha I(\kappa_{nl}\,\varsigma_1, \kappa_{nl}\,\varsigma_2, \kappa_{nc}\,\varsigma_3) \tag{13}$$

where

$$\kappa_{nl} = \frac{1}{\pi\eta}\hat{T}\sin\left(\frac{\vartheta\Lambda}{2\eta ts}\right) g(\vartheta,\varphi), \tag{14a}$$

$$\kappa_{nc} = \frac{1}{\pi\eta}\hat{T}\cos\left(\frac{\vartheta\Lambda}{2\eta ts}\right) h_s\left(\mathrm{sinc}^2\frac{\vartheta}{2} - \mathrm{sinc}\vartheta\right)\vartheta \tag{14b}$$

are the coupling coefficients between the polarization of the seed photon and that of the laser pulse in the NBW process, and

$$g(\vartheta,\varphi) = \cos\vartheta + \mathrm{sinc}^2\frac{\vartheta}{2} - 2\mathrm{sinc}\,\vartheta + \frac{1}{\varsigma_l}\left(1 + \mathrm{sinc}^2\frac{\vartheta}{2} - 2\mathrm{sinc}\,\vartheta\right)\cos 2\varphi.$$

Λ is the Kibble mass and expressed as [53]

$$\Lambda = 1 + I - I\mathrm{sinc}^2\frac{\vartheta}{2} - I\varsigma_l\cos 2\varphi\left(\mathrm{sinc}^2\frac{\vartheta}{2} - \mathrm{sinc}\vartheta\right)$$

depending on the laser power density $I = \xi^2(1+\delta^2)/2$ and its linear-polarization degree ς_l. $\hat{T}$ is the integral operator given as

$$\hat{T} = \int_0^1 \mathrm{d}s \int_{-\infty}^{\infty}\mathrm{d}\varphi \int_0^{\infty}\frac{\mathrm{d}\vartheta}{\vartheta},$$

with the average phase $\varphi = (\phi_1 + \phi_2)/2$ and the interference phase $\vartheta = \phi_1 - \phi_2$ [54–56].

As we can see, in the NBW process, the polarization contribution n_i is proportional directly to the corresponding

laser Stokes parameter ς_i, as discussed in Figs. 3 and 4, with the coupling coefficients in (14) depending not only on the laser power, but also on the field ellipticity. The two linear-polarization components share, again, the same coupling coefficient because of the symmetry of rotating the linear-polarization axis as discussed in Fig. 3. We put the fine structure constant α out of the coupling coefficients as the NBW process is a single-vertex process, and I is because of the increase of the contributions with the laser power and in the perturbative regime $n_i \propto \xi^2$ in (5).

C. Optimal photon polarization

Based on the above discussions, the optimal polarization of the seed photon (4) for the NBW process can be written as

$$(\Gamma_1, \Gamma_2, \Gamma_3) = \hat{\kappa}_{nl} \frac{(\varsigma_1, \varsigma_2, \sigma_n \varsigma_3)}{(\varsigma_1^2 + \varsigma_2^2 + \sigma_n^2 \varsigma_3^2)^{1/2}} \tag{15}$$

based on the polarization of the laser pulse, where $\hat{\kappa}_{nl} = -1$ is the sign of κ_{nl} acquired numerically, and $\sigma_n = \kappa_{nc}/\kappa_{nl}$ denotes the difference between the coupling coefficients κ_{nl} and κ_{nc}. If $\sigma_n \neq 1$, the photon's optimal polarization state would deviate from the orthogonal state $-(\varsigma_1, \varsigma_2, \varsigma_3)$ of the laser polarization.

In Fig. 5(a), we present the dependence of the coupling coefficients κ_{nl} and κ_{nc} on the field ellipticity calculating from the finite-pulse results in Fig. 4(b). As shown, the values of κ_{nl} and κ_{nc} vary slightly with the change of the field ellipticity δ, and there exists significant difference between κ_{nl} and κ_{nc} with the ratio $\sigma_n < 1$, which also changes for different δ. Therefore, the optimal polarization state of the seed photon, for the maximal yield, is much different from the orthogonal state $-(\varsigma_1, \varsigma_2, \varsigma_3)$ of the laser polarization as one can see in Fig. 5(b), except in the regions around $\delta \approx 0$, 1, where the laser is linearly and circularly polarized, respectively. With the optimized photon polarization in Fig. 5(b), the production yield could be enhanced by more than 20% compared to the unpolarized case as shown in Fig. 4(a).

The dependence of κ_{nl} and κ_{nc} on the laser power density is presented in Fig. 6(a) for the fixed field ellipticity $\delta = 0.5$ and deflection angle $\theta = \pi/8$. As shown, in the low-power density region $I < 10^{-3}$, κ_{nl} and κ_{nc} are independent of the laser power I because the LBW process dominates the production, and κ_{nl} and κ_{nc} can be acquired alternatively from the perturbative result (5) with κ_l and κ_c depending only on the parameter β. The values of κ_{nl} and κ_{nc} are

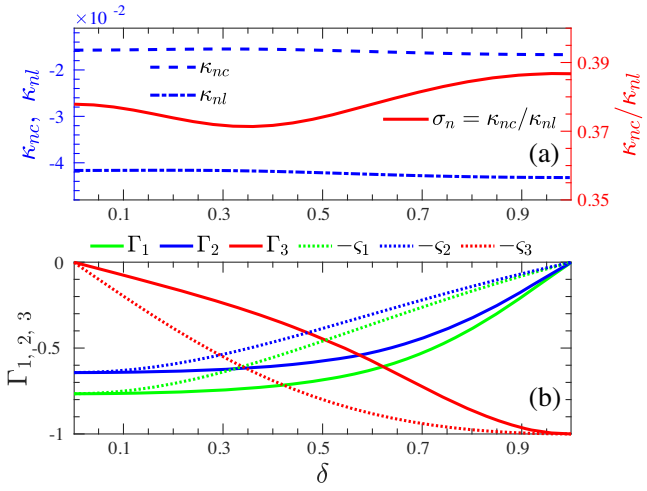

FIG. 5. (a) The variation of the coupling coefficients κ_{nl}, κ_{nc} with the change of the field ellipticity. The ratio $\sigma_n = \kappa_{nc}/\kappa_{nl}$ is also plotted with the right y-axis. The coefficient κ_{nl} calculated from n_1 is exactly the same as that from n_2. (b) The Stokes parameters of the photon's optimal polarization in (3) for different δ. We also show the comparison with the orthogonal state $-(\varsigma_1, \varsigma_2, \varsigma_3)$ of the laser polarization. The same parameters as in Fig. 4 are used.

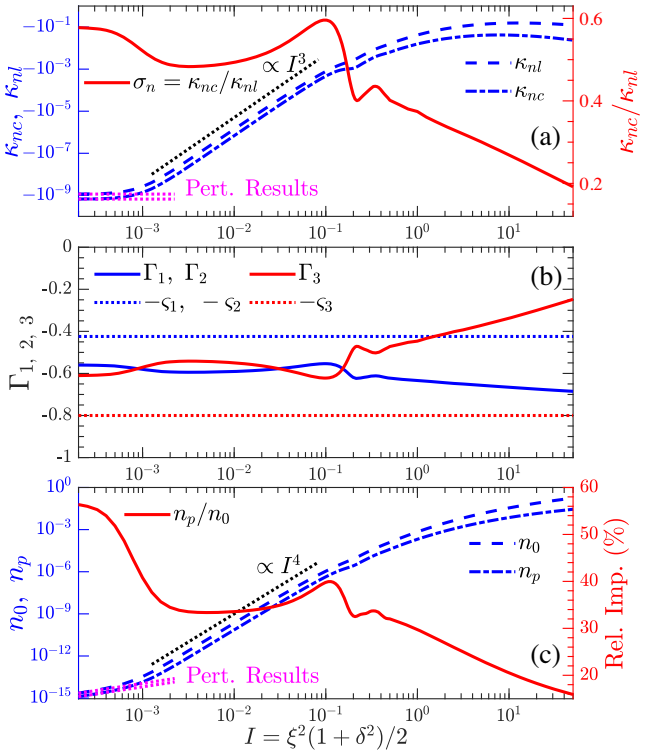

FIG. 6. (a) The variation of the coupling coefficients κ_{nl}, κ_{nc} with the increase of the laser power density. The dependence of the ratio $\sigma_n = \kappa_{nc}/\kappa_{nl}$ on the laser power is also presented with the right y-axis. (b) The Stokes parameters of the photon's optimal polarization with the change of the laser power. $\Gamma_1 = \Gamma_2$ as the field deflection angle is $\theta = \pi/8$. (c) The yield from the unpolarized contribution n_0 and the maximal polarization contribution n_p, and the relative importance of the polarization effect n_p/n_0. In (a) and (b), the pink dotted lines are the corresponding perturbative results acquired from (5), and the black dotted lines show the varying trend of the curves. The field ellipticity is $\delta = 0.5$. The other parameters are the same as in Fig. 4.

determined by the energy parameter η and the pulse envelope. In this region, the positron yield increases as $n_0, n_p \propto I$ shown in Fig. 6(c) because of the single-photon effect with the high-frequency components from the finite-pulse effect [23]. In the intermediate laser power region $10^{-3} < I < 10^{-1}$, the coupling coefficients increase as $\kappa_{nl}, \kappa_{nc} \propto I^3$ because of the multiphoton perturbative effect, in which $4 = \lceil 2/\eta \rceil$ laser photons are involved in the production process and the positron yield increases in the trend as $n_0, n_p \propto I^4$ in Fig. 6(c), where $\lceil x \rceil$ denotes the minimal integer larger than x. With the further increase of the laser power $I \gtrsim 0.5$, this four-photon channel is forbidden and a higher number of laser photons $n = \lceil 2(1+I)/\eta \rceil$ would be involved in the production process. Therefore, the fully nonperturbative effect would be dominant. The increase of the coupling coefficients κ_{nl} and κ_{nc} becomes slower, as well as the increase of the positron yield in Fig. 6(c). In Fig. 6(a), we can also see the evident difference between κ_{nl} and κ_{nc} in the broad laser power region with the ratio σ_n much smaller than 1 and depending also sensitively on the laser power.

In Fig. 6(b), the optimal polarization state of the seed photon is presented with the change of the laser power. Because the field deflection angle is $\theta = \pi/8$, the two linear-polarization components are equal, $\Gamma_1 = \Gamma_2$. As shown, the photon's optimal polarization state deviates considerably from the orthogonal state of the laser polarization. Especially in the nonperturbative regime $I > 0.5$, the circular-polarization degree $|\Gamma_3|$ of the optimal polarization decreases rapidly with the increase of I, because of the rapid decrease of the ratio σ_n for larger I in Fig. 6(a), which means that the contribution from the circular polarization becomes less important. In the ultrahigh-intensity regime $\xi \gg 10$ (not shown in Fig. 6), in which the locally constant field approximation would work precisely [33,56], the contribution from the circular polarization would be negligible, i.e., $k_{nc} \to 0$ and $\Gamma_3 \to 0$. This is because the formation length of the NBW process becomes much shorter than the typical length of the field variation [57] and the laser pulse would work as a linearly polarized field with the direction varying with the laser phase [33].

With the polarization-optimized seed photon, the positron yield could be enhanced appreciably as shown in Fig. 6(c). In the perturbative intensity regime $I < 10^{-3}$, the positron yield could be enhanced more than 55% by the polarization effect compared with the unpolarized case, and in the multiphoton perturbative regime $10^{-3} < I < 10^{-1}$, the yield enhancement is about 34% from the optimized polarization state. With the further increase of the laser power, even though the relative importance of the polarization contribution becomes less, the positron yield could still be improved more than 16% at $I \lesssim 50$.

V. CONCLUSION

The optimization of the photon polarization state to the maximal positron yield of the Breit-Wheeler pair production is investigated in arbitrarily polarized plane wave backgrounds for a broad intensity region. Both the polarization of the photon and the laser pulse are comprehensively described with the classical Stokes parameters.

The optimal polarization state of the seed photon is the result of the polarization coupling with the laser pulse/photons in the production process. For the laser pulse with the pure linear or circular polarization, the seed photon's optimal polarization is the orthogonal state of the laser pulse. However, because of the evident difference between the coupling coefficients for the linear- and circular-polarization components, the seed photon's optimal polarization state in an elliptically polarized laser background deviates considerably from the orthogonal state of the laser polarization, especially in the ultrahigh-intensity regime in which the linear-polarization coupling coefficient is much larger than that of the circular polarization and thus the seed photon's optimal polarization would tend to the linear polarization.

With the polarization-optimized seed photon, the positron yield could be considerably enhanced in a broad intensity region. For the laser intensity region $\xi \sim \mathcal{O}(1)$ of current laser-particle experiments, the yield enhancement from the optimized photon polarization could be more than 20% compared to the unpolarized case.

ACKNOWLEDGMENTS

The authors thank A. Ilderton for useful suggestions and comments on the manuscript. The authors acknowledge the support from the National Natural Science Foundation of China, Grant No. 12104428. The work was carried out at Marine Big Data Center of Institute for Advanced Ocean Study of Ocean University of China.

[1] G. Breit and J. A. Wheeler, Phys. Rev. **46**, 1087 (1934).
[2] V. N. Baier and A. G. Grozin, arXiv:hep-ph/0209361.
[3] J. Adam, L. Adamczyk, J. R. Adams, J. K. Adkins, G. Agakishiev, M. M. Aggarwal, Z. Ahammed, I. Alekseev, D. M. Anderson, A. Aparin *et al.* (STAR Collaboration), Phys. Rev. Lett. **127**, 052302 (2021).
[4] H. R. Reiss, J. Math. Phys. (N.Y.) **3**, 59 (1962).
[5] A. Di Piazza, C. Müller, K. Z. Hatsagortsyan, and C. H. Keitel, Rev. Mod. Phys. **84**, 1177 (2012).

[6] A. Gonoskov, T. G. Blackburn, M. Marklund, and S. S. Bulanov, arXiv:2107.02161.
[7] A. Fedotov, A. Ilderton, F. Karbstein, B. King, D. Seipt, H. Taya, and G. Torgrimsson, arXiv:2203.00019.
[8] D. L. Burke, R. C. Field, G. Horton-Smith, J. E. Spencer, D. Walz, S. C. Berridge, W. M. Bugg, K. Shmakov, A. W. Weidemann, C. Bula *et al.*, Phys. Rev. Lett. **79**, 1626 (1997).
[9] C. Bamber, S. J. Boege, T. Koffas, T. Kotseroglou, A. C. Melissinos, D. D. Meyerhofer, D. A. Reis, W. Ragg, C. Bula, K. T. McDonald *et al.*, Phys. Rev. D **60**, 092004 (1999).
[10] A. Nikishov and V. Ritus, Sov. Phys. JETP **19**, 529 (1964), http://83.149.229.155/cgi-bin/dn/e_019_02_0529.pdf.
[11] T. Heinzl, A. Ilderton, and M. Marklund, Phys. Lett. B **692**, 250 (2010).
[12] K. Krajewska and J. Z. Kamiński, Phys. Rev. A **86**, 052104 (2012).
[13] A. I. Titov, H. Takabe, B. Kämpfer, and A. Hosaka, Phys. Rev. Lett. **108**, 240406 (2012).
[14] A. M. Fedotov and A. A. Mironov, Phys. Rev. A **88**, 062110 (2013).
[15] A. I. Titov, B. Kämpfer, A. Hosaka, T. Nousch, and D. Seipt, Phys. Rev. D **93**, 045010 (2016).
[16] M. J. A. Jansen and C. Müller, Phys. Rev. A **88**, 052125 (2013).
[17] M. J. Jansen and C. Mller, Phys. Lett. B **766**, 71 (2017).
[18] A. I. Titov, H. Takabe, and B. Kämpfer, Phys. Rev. D **98**, 036022 (2018).
[19] A. Ilderton, Phys. Rev. D **100**, 125018 (2019).
[20] A. Ilderton, Phys. Rev. D **101**, 016006 (2020).
[21] B. King, Phys. Rev. A **101**, 042508 (2020).
[22] S. Tang, Phys. Rev. A **104**, 022209 (2021).
[23] S. Tang and B. King, Phys. Rev. D **104**, 096019 (2021).
[24] D. Y. Ivanov, G. Kotkin, and V. Serbo, Eur. Phys. J. C **40**, 27 (2005).
[25] V. Katkov, J. Exp. Theor. Phys. **114**, 226 (2012).
[26] Y.-F. Li, R. Shaisultanov, Y.-Y. Chen, F. Wan, K. Z. Hatsagortsyan, C. H. Keitel, and J.-X. Li, Phys. Rev. Lett. **124**, 014801 (2020).
[27] Y.-Y. Chen, K. Z. Hatsagortsyan, C. H. Keitel, and R. Shaisultanov, Phys. Rev. D **105**, 116013 (2022).
[28] V. Dinu and G. Torgrimsson, Phys. Rev. D **102**, 016018 (2020).
[29] G. Torgrimsson, New J. Phys. **23**, 065001 (2021).
[30] T. N. Wistisen, Phys. Rev. D **101**, 076017 (2020).
[31] A. I. Titov and B. Kämpfer, Eur. Phys. J. D **74**, 218 (2020).
[32] D. Seipt and B. King, Phys. Rev. A **102**, 052805 (2020).
[33] S. Tang, Phys. Rev. D **105**, 056018 (2022).
[34] H. Abramowicz *et al.*, Eur. Phys. J. Special Topics **230**, 2445 (2021).
[35] M. Borysova, J. Instrum. **16**, C12030 (2021).
[36] A. J. Macleod, J. Phys. Conf. Ser. **2249**, 012022 (2022).
[37] R. Jacobs, SciPost Phys. Proc. **8**, 088 (2022).
[38] S. Meuren, in *Proceedings of the Third Conference on Extremely High Intensity Laser Physics (ExHILP)* (2019), https://conf.slac.stanford.edu/facet-2-2019/sites/facet-2-2019.conf.slac.stanford.edu/files/basic-page-docs/sfqed_2019.pdf.
[39] B. Naranjo, G. Andonian, N. Cavanagh, A. D. Piazza, A. Fukasawa, E. Gerstmayr, R. Holtzapple, C. Keitel, N. Majernik, S. Meuren *et al.*, in *Proceedings of the International Particle Accelerator Conference (12th)* (JACoW Publishing, Geneva, 2021), https://jacow.org/ipac2021/papers/thpab270.pdf.
[40] F. C. Salgado, N. Cavanagh, M. Tamburini, D. W. Storey, R. Beyer, P. H. Bucksbaum, Z. Chen, A. Di Piazza, E. Gerstmayr, Harsh *et al.*, New J. Phys. **24**, 015002 (2021).
[41] S. Meuren, P. H. Bucksbaum, N. J. Fisch, F. Fiúza, S. Glenzer, M. J. Hogan, K. Qu, D. A. Reis, G. White, and V. Yakimenko, arXiv:2002.10051.
[42] A. Di Piazza, Phys. Rev. A **91**, 042118 (2015).
[43] A. Di Piazza, Phys. Rev. Lett. **117**, 213201 (2016).
[44] A. Di Piazza, Phys. Rev. A **95**, 032121 (2017).
[45] A. Di Piazza, Phys. Rev. D **103**, 076011 (2021).
[46] V. N. Baier, A. I. Mil'shtein, and V. M. Strakhovenko, J. Exp. Theor. Phys. **42**, 961 (1976), http://jetp.ras.ru/cgi-bin/dn/e_042_06_0961.pdf.
[47] V. B. Berestetskii, E. M. Lifshitz, and L. P. Pitaevskii, *Quantum Electrodynamics*, 2nd ed. (Butterworth-Heinemann, Oxford, 1982).
[48] J. D. Jackson, *Classical Electrodynamics* 3rd ed. (Wiley, New York, 1999).
[49] Y. J. Ng and W.-y. Tsai, Phys. Rev. D **16**, 286 (1977).
[50] W. Greiner and J. Reinhardt, *Quantum Electrodynamics* 4th ed. (Springer, Berlin, 2009).
[51] B. King and S. Tang, Phys. Rev. A **102**, 022809 (2020).
[52] T. Heinzl, B. King, and A. J. MacLeod, Phys. Rev. A **102**, 063110 (2020).
[53] L. S. Brown and T. W. B. Kibble, Phys. Rev. **133**, A705 (1964).
[54] V. Dinu, C. Harvey, A. Ilderton, M. Marklund, and G. Torgrimsson, Phys. Rev. Lett. **116**, 044801 (2016).
[55] D. Seipt, arXiv:1701.03692.
[56] A. Ilderton, B. King, and D. Seipt, Phys. Rev. A **99**, 042121 (2019).
[57] V. I. Ritus, J. Russ. Laser Res. **6**, 497 (1985).